

The Effect of DLC Coating Thickness on Elastohydrodynamic Friction

M. Björling · R. Larsson · P. Marklund

Received: 1 April 2014 / Accepted: 11 June 2014 / Published online: 22 June 2014
© The Author(s) 2014. This article is published with open access at Springerlink.com

Abstract The application of surface coatings has been shown to reduce friction in elastohydrodynamic lubrication (EHL), not only in the mixed and boundary regime when asperity interactions occur, but also in the full film regime. Several studies suggest that the full film friction reduction is due to a violation of the no-slip boundary condition and thus slip is taking place between the solid and the liquid. Another hypothesis proposes that the full film friction reduction is due to the low thermal conductivity of diamond-like carbon (DLC) coatings. In this work, two DLC coatings with the same composition, but different thicknesses, are investigated with uncoated steel specimens as a reference, all with the same surface roughness. Friction tests in a ball-on-disk machine show that both coatings reduce friction compared to the uncoated reference case in full film EHL. The thicker coating is significantly more effective at reducing friction than the thinner one at a maximum friction reduction of 41 % compared to 29 % for the thinner coating. Moreover, contact angle measurements, surface energy measurements, and spreading parameter calculations show no statistically significant differences between the two coatings, suggesting that the friction reduction capabilities of coatings in full film EHL cannot be described by solid–liquid interactions alone. The difference in friction reduction between the specimens in this work is mainly attributed to different thermal properties.

Keywords Diamond-like carbon (DLC) · EHL · Thermal conductivity · Friction · Thermal effects · Surface energy

List of symbols

γ_l^D	Dispersive component of surface tension (N/m)
γ_s^D	Dispersive component of surface energy (J/m ²)
γ_l^P	Polar component of surface tension (N/m)
γ_s^P	Polar component of surface energy (J/m ²)
γ_l	Total surface tension (N/m)
θ	Contact angle (deg)
A_t	Heat transfer area (m ²)
c	Coating thickness (m)
dT	Temperature difference across coating (K)
k	Thermal conductivity (W/mK)
q_t	Heat transfer (W)

1 Introduction

Surface engineering has emerged as an important part in reducing friction in the field of elastohydrodynamic lubrication (EHL). Smoother surfaces in contact have the advantage of pushing the transition from full film lubrication to mixed lubrication toward lower speeds and will thus lead to reductions in both friction and wear. Furthermore has the use of tribological coatings grown substantially in the last decade to provide various enhancements such as lower friction and wear both in dry and lubricated contacts. Diamond-like carbon (DLC) coatings are the subject of many studies since they possess properties such as low friction characteristics, high wear and corrosion resistance, chemical inertness, thermal stability, as well as high hardness and high elastic modulus. DLC coatings generally reduce friction in boundary and mixed lubrication regimes

M. Björling (✉) · R. Larsson · P. Marklund
Division of Machine Elements, Department of Engineering
Science and Mathematics, Luleå University of Technology,
97187 Luleå, Sweden
e-mail: marcus.bjorling@ltu.se

by lowering the contact friction between the asperities. However, the matter of interest in this paper is the reduction that is achieved by DLC coatings in full film EHL where there is no contact between the surfaces and the lubricant carries all of the load. Several authors have experimentally observed a reduction in friction with DLC-coated surfaces in full film EHL [6, 7, 14, 27, 48]. The friction reduction has been explained by several authors as an effect of boundary slip, or solid–liquid interface slip [14, 27, 29] a phenomena thoroughly discussed in literature [12, 25, 37, 38, 41, 42, 46, 47, 49], where some of the work is based on atomically smooth surfaces.

However, it is still not entirely clear how the mechanism of slip works, and several hypothesis can be found in the literature. In many cases, poor wetting or high contact angle is proposed as the main feature to promote slip [13, 23, 25, 29, 41, 42, 49] and in other cases low surface energy [14, 27]. However, using only surface energy as a means to determine the potential of solid–liquid slip may not be suitable since surface energy is a material property and tells nothing about the interaction of a specific material with a specific fluid. On the other hand, contact angle measurements represent a property of the specific surface and lubricant combination and could intuitively seem to be more suitable. However, Kalin and Polajnar have recently published studies including many different lubricants and coatings where the influence of surface energy and contact angle is discussed [26, 28]. They conclude that contact angle cannot be used in isolation to predict the wetting behavior and instead propose the use of a spreading parameter which correlates well with the surface energy. They also showed the correlation between contact angle, surface energy, and spreading parameter with friction coefficients in full film EHL, where, especially, the spreading parameter and the polar part of the surface energy correlate very well with the friction measurements [27].

Furthermore, many authors have concluded that for solid–liquid slip to take place, the surfaces have to be very smooth, generally below 6 nm RMS [12, 41, 42, 50]. However, the present authors have presented an investigation in which friction reduction with DLC coatings was measured [7] in full film EHL even when the combined RMS roughness of the surfaces was in the range of 155–355 nm. Based on a simplified analytical estimation of the temperature increase in the lubricant film induced by DLC surface coating, the authors proposed that the friction reduction could be a result of thermal insulation due to the low thermal conductivity observed for some DLC coatings [2, 31, 40]. The temperature increase in the lubricant film would reduce the viscosity and thereby reduce the coefficient of friction. In a more recent study [6], the present authors used a more advanced and thoroughly validated [5, 20–22] 3D numerical model to predict the effect of thin

insulating layers on full film elastohydrodynamic (EHD) friction to be compared with experimental measurements. The presented simulations, validated by experiments, showed that applying a thin diamond-like carbon coating to metal surfaces creates an insulating effect that, due to the increased liquid lubricant film temperature at the center of the contact, locally reduces lubricant viscosity and thus friction. This model was later refined by Habchi and used to numerically investigate the effect of different coating thickness and thermal properties on EHD friction [19].

In this work, specimens coated with the same DLC coating, but with different coating thickness, are investigated in terms of friction reduction in full film EHL and compared to measurements of contact angle and surface energy of the coatings. By investigating two coatings with supposedly the same surface energy and contact angle, but with different thicknesses and hence thermal properties, the authors want to provide further information about the mechanisms behind the full film EHD friction reduction capabilities of DLC coatings.

2 Overall Methodology

The following sections cover the test specimens, lubricant, and coatings used. It also contains information about how the experimental equipment for the friction tests is set up, and how the experiments are performed. Finally, the procedure for the contact angle, surface energy, and surface tension measurements are discussed.

2.1 Test Specimens and Lubricant

The tests were performed with a commercially available DLC coating produced with two different thicknesses and uncoated DIN 100Cr6 (AISI 52100) bearing steel as a reference. For the friction tests in the ball-on-disk machine, polished balls and disks were used that had been measured to a surface roughness, RMS of 25 nm for the balls and 35 nm for the disks, which gives a combined roughness of approximately 43 nm. These roughness values were also maintained after the specimens had been coated with DLC. The surface roughness measurements were conducted in a Wyko NT1100 optical profilometer system from Veeco. The measurements were performed using 10x magnification and 1x field of view. The balls are grade 20 with a 13/16 inch (20.63 mm) outer diameter and a hardness of about 60 HRC. The disks have a 4 inch (101.6 mm) outer diameter, a circumferential grind (before polish) and are through hardened to about 60 HRC. Except the steel uncoated reference specimens, the remaining specimens were coated with Tribobond 43, a hydrogenated amorphous carbon ((Cr+)a-C:H), through plasma-assisted chemical

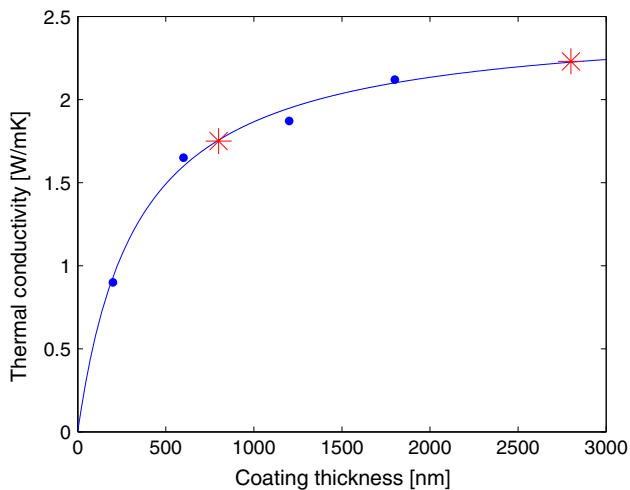


Fig. 1 Thermal conductivity with respect to coating thickness for a-C:H coating. The dots represent the measured values used for the curve fit. The stars represent the values for the coating thicknesses in this paper

vapor deposition. The specimens were prepared with two different coating thicknesses, 0.8 and 2.8 μm , measured using calotest. A chromium-based interlayer with a thickness of 0.1–0.3 μm deposited by magnetron sputtering was used to improve the adhesion. The thermal conductivities were not measured on these specific coatings, but approximated by the formula obtained by Kim et al. [31] that is expressed in Fig. 1. The dots represents the actual measurements performed by Kim et al. from which they derived the curve fit. The stars represent the coating thicknesses used in this work. Other work has been performed focusing on measuring thermal conductivities of DLC coatings thinner than 20 nm where a thermal conductivity of 0.09 W/mK was obtained for a coating of approximately 3 nm [2]. The effect of thermal boundary resistance [43] is more influential at thinner coating thicknesses and is the most likely explanation why the thermal conductivity has a rapid decrease for thinner coatings. It is also likely that the chromium interlayer will further reduce the thermal conductivity due to additional thermal boundary resistance. The thermal conductivities are expected to be around 1.75 and 2.23 W/mK for the 0.8 and 2.8 μm coatings, respectively. This should be compared to a value of 46.6 W/mK for the substrate material. Note that even though the thermal conductivity is higher for the thicker coating, the total thermal insulating effect is still higher due to the increase in coating thickness. Consider Fourier's law of thermal conductive heat transfer:

$$q_t = kA_t dT/c \quad (1)$$

where q_t is the heat transfer, k is the thermal conductivity, A_t is the heat transfer area, dT is the temperature difference across the material, and c is the coating thickness.

Assuming identical values for A_t and dT for the different coating thicknesses would give approximately 2.75 times as much heat conducted through the thinner coating.

The lubricant used for the tests was squalane, a commercially available low molecular weight (422.81 g/mol) branched alkane (2,6,10,15,19,23-hexamethyltetracosane). A lubricant without additives was chosen to minimize the effect of tribochemical reactions on the friction coefficient. At the test temperature of 40 $^{\circ}\text{C}$, the ambient viscosity of squalane is 15 mPas, and the pressure viscosity coefficient is 18 GPa^{-1} [1].

2.2 Ball-on-Disk Tribotester

The experiments were carried out with a Wedeven Associates Machine (WAM) 11, ball-on-disk test device. The lubricant is supplied at the center of the disk in an oil dispenser that distributes the lubricant across the disk surface. The lubricant is circulated in a closed loop from the oil bath, through a peristaltic pump to the oil dispenser at the center of the disk. The peristaltic pump is delivering approximately 180 ml/min. Three thermocouples are used in the test setup, one located in the oil bath, one in the outlet of the oil supply, and one trailing in the oil film close to the inlet region of the ball-on-disk contact. A more thorough description of the test rig and its features is presented in previous work [8].

2.3 Test Procedure

In this investigation, we only tested the combination of uncoated specimens, specimens coated with 0.8 μm DLC, and specimens coated with 2.8 μm DLC. Previous investigations have shown that a coating on only one of the specimens in contact still gives a reduction in friction, but not as great as if both specimens are coated [7, 27]. The ball-on-disk test device was used to generate friction data from a series of tests under different operating conditions. In each test, the entrainment speed and contact pressure were held constant while the slide to roll ratio (SRR) was varied from 0.0002 to 1.05. SRR is defined as the ball surface speed subtracted by the disk surface speed giving the sliding speed. The sliding speed is then divided with the entrainment speed giving SRR. All tests in this investigation were hence conducted with the ball having a higher surface speed than the disk. Both ball and disk specimens were cleaned with heptane and ethyl alcohol before starting the experiments for each of the test cases. Before starting the experiments for each test case, the test device was warmed up to the desired operating temperature during approximately 60 min with lubricant circulation over both ball and disk to ensure thermal stability. When a stable temperature was reached, an 80 N or a 300 N load was

Table 1 Investigated conditions

Temperature	40 °C
Contact load	80 and 300 N
Maximum hertzian pressure	1.25 and 1.94 GPa
Entrainment speed, U_e	1.611, 3.145 and 6.144 m/s
Slide to roll ratio, SRR	0.0002–1.05
Coating thickness	0.8 and 2.8 μm

applied which is equivalent to 1.25 or 1.94 GPa maximum Hertzian pressure and the machine was calibrated for pure rolling by adjusting spindle angle and positioning of the ball to ensure a condition of no spinning. These settings were then held constant for 20 min to ensure a mild run-in. Subsequently, the test cycle was started, wherein the entrainment speed was kept at a constant value, and the slide to roll ratio was varied from the lowest to the highest value. The test cycle was repeated seven times for each entrainment speed. The temperature of the oil bulk and fluid adhered at the disk surface was typically deviating less than ± 1.5 °C from the target temperature of 40 °C during testing. Four different entrainment speeds were used in the tests. The entrainment speeds were chosen such that the minimum film thickness in the most severe case (lowest entrainment speed and highest SRR with the thickest coating) would still be higher than the combined roughness of the specimens and thus still be in the full film regime. The film thickness for 1.25 GPa, an entrainment speed of 1.6 m/s, and 1.04 in SRR give an uncoated minimum film thickness of 65 nm, while the coated case would give a minimum film thickness of 63 nm. The film thickness calculations were made with the numerical model used in a previous investigation including the effect of a thermally insulating coating on film thickness and friction in EHL [6]. Here, along with another numerical work [19], it is concluded that although a thermally insulating coating could have a significant effect on friction, the film thickness is barely affected. A summary of the investigated conditions can be seen in Table 1.

2.4 Surface Energy and Wetting

The surface energies of the specimens were evaluated using the Owens-Wend-Rabel-Kaelbe (OWRK) method (Eq. 2) [35]. This method requires contact angle measurements of the specimens with at least two liquids with known properties. In this investigation, demineralized water and diiodomethane were used. The properties of these fluids needed for the OWRK method, total surface tension, and the dispersive and polar components of surface tension obtained from literature [15] are presented in Table 2. It should be mentioned that several theoretical models exist for the calculation of surface energy from contact

Table 2 Surface tension and its polar and dispersive components for test liquids

Liquid	Total surface tension γ_l (mN/m)	Dispersive component γ_l^D (mN/m)	Polar component γ_l^P (mN/m)
Water	72.8	21.80	51.00
Diiodomethane	50.8	50.8	0
Squalane	31.8	30.7	1.1

angle measurements. Kalin and Polajnar [26, 28] recently investigated the surface energies of several different DLC coatings using OWRK, Oss and Wu methods. They concluded that these three models were qualitatively the same (for the samples and fluids they used), providing the same ranking of the surfaces, but with a difference in absolute values ranging between 5 and 25 %. The OWRK method, Eq. 2, presented values in between the Oss method and the Wu method and is probably the most used model in literature that is why it is used also in this investigation.

$$\gamma_l(1 + \cos\theta) = 2 \left(\sqrt{\gamma_s^D \gamma_l^D} + \sqrt{\gamma_s^P \gamma_l^P} \right) \quad (2)$$

where γ_l is the total surface tension of the fluid, θ the contact angle, γ_s^D the dispersive component of surface energy, γ_s^P the polar component of surface energy, γ_l^D the dispersive component of surface tension and γ_l^P the polar component of surface tension.

The contact angle measurements were conducted with the sessile drop technique using an optical goniometer, Fibro 1121/1122 DAT-Dynamic Absorption and Contact Angle Tester. Before the measurements were conducted, the specimens were cleaned with acetone and ethanol and dried in a stream of hot air. The drop size was 2.5 μm and used for all lubricants for consistency. At this small volume, the effect of the drops impact due to its weight can be ignored [34]. Each fluid and liquid combination was repeated at least 8 times before the average value was calculated. The contact angle of the lubricant typically changed with time after having been deposited on the surface. The value was measured after 12 s for both reference fluids and all materials for consistency. In the case of squalane that showed contact angles that changed more with time, the measurement was done after 16 s.

2.5 Surface Tension

The surface tension of the lubricant used for the friction tests was determined using the same optical goniometer as for the contact angle measurements. The pendant drop method was used to establish the surface tension. Each test was repeated 5 times, and the average value was calculated. Since the pendant drop method only gives the total surface

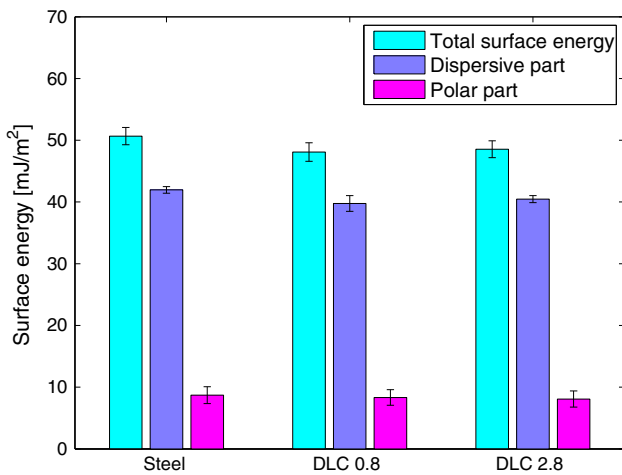


Fig. 2 Surface energies and the corresponding dispersive and polar parts of investigated surfaces determined using the OWRK method

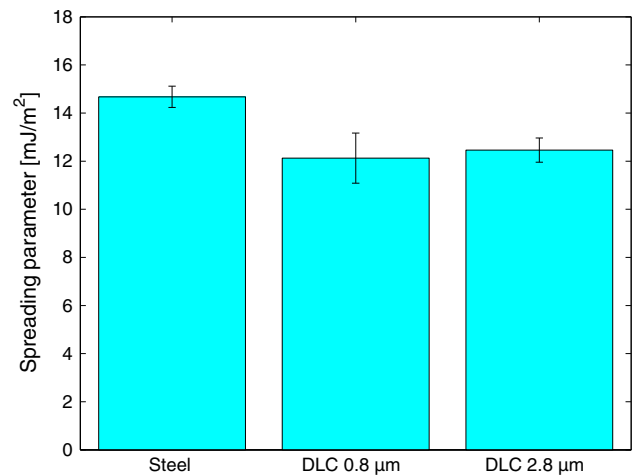


Fig. 3 Spreading parameter values for squalane and the investigated surfaces

energy of the lubricant, another method is needed to determine the polar and dispersive components of the surface tension. By measuring the contact angle for the specific lubricant on PTFE, the dispersive component of the surface tension can be acquired. This is because PTFE only has a dispersive component of surface energy, 23.53 mJ/m², and consequently, the OWRK method could be used to calculate the dispersive component of the surface tension. The polar part is then calculated using Fowkes method [16] with the following equation:

$$\gamma_l = \gamma_l^D + \gamma_l^P \tag{3}$$

2.6 Spreading Parameter

Kalin and Polajnar proposed the use of a spreading parameter for evaluating the wetting between a surface and a lubricant [27]. They found that while contact angle measurements did not correlate with the friction reduction, the spreading parameter did. Combining the Young equation and the OWRK model, they derived a spreading parameter that was used to characterize the spreading of the surface and liquid combinations investigated in this article:

$$S_p = 2 \left[\sqrt{\gamma_s^D \gamma_l^D} + \sqrt{\gamma_s^P \gamma_l^P} - \gamma_l \right] \tag{4}$$

3 Results

The surface energies for the investigated specimens are presented in Fig. 2. It shows that uncoated steel has the highest surface energy of 50.7 mJ/m², while the DLC coatings have 48.1 and 48.5 mJ/m², respectively, for the 0.8 and 2.8 μm coatings. When looking at the distribution in dispersive and polar components of the surface energies for the investigated surfaces, they are all very similar in the sense that the dispersive component of the surface energy

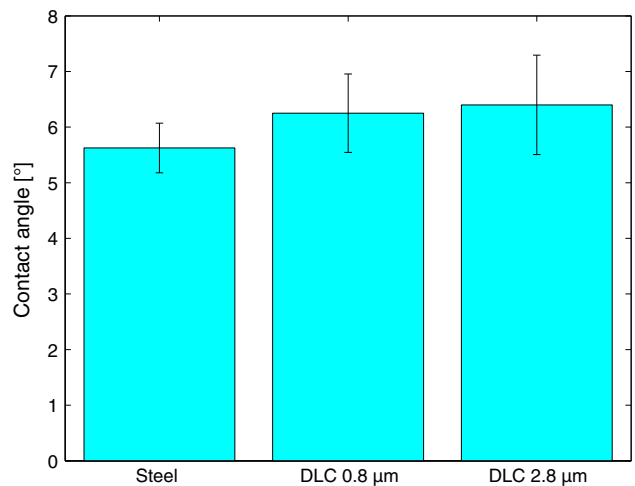


Fig. 4 Contact angle for squalane on the investigated surfaces

is dominant and only a small part is coming from the polar component.

Figure 3 shows the results for the calculated spreading parameters for the combination of squalane and the different surfaces. The spreading parameter defined by Kalin and Polajnar [27], Eq. 4, represents the wetting behavior of the lubricant and surface combinations. In all cases, the spreading parameter is positive, suggesting that the lubricant spreads over the surfaces with time and does not obtain a constant contact angle immediately. According to the equation, the lubricant will spread most easily on the uncoated steel surface and less on the coated surfaces. In this case, the thicker coating has a slightly higher spreading parameter suggesting that it would provide lower wetting of the surface with squalane compared to the thinner coating.

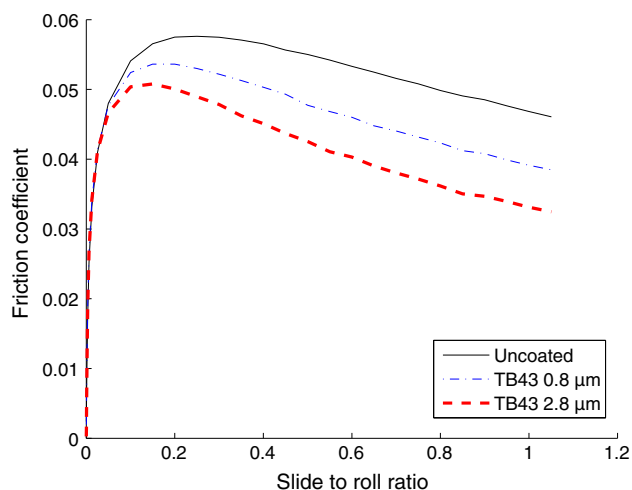


Fig. 5 Friction measurements for squalane at 1.6 m/s entrainment speed and 1.25 GPa of maximum hertzian pressure for uncoated steel and two different thicknesses of the same DLC coating

Figure 4 shows the results from the contact angle measurements for squalane on the specimens. The values were taken after about 16 s and represent a steady-state contact angle. The low contact angles indicate good wetting on all specimens.

Figures 5, 6, 7 show the results from the ball-on-disk friction measurements with the uncoated specimens and the two different coating thicknesses. Although three different entrainment speeds were investigated at 1.25 GPa pressure (Table 1), only the lowest and highest entrainment speeds are shown here since the intermediate entrainment speed showed the same trends as the two presented here. For 1.94 GPa, only the highest entrainment speed case is shown here as a comparison with the 1.25 GPa case at the same speed. Table 3 shows the reduction in friction for all investigated cases at the highest SRR of 1.05. Table 3 also shows that in general, the percental friction reduction is greater for the lower pressure independent of coating thickness and entrainment speed.

It is clear that the uncoated specimens have the highest friction coefficients for all tested combinations of pressures and entrainment speeds. The thinner DLC coating leads to a significant reduction in friction coefficient, and the friction is further reduced for the specimens with the thicker coating. For all entrainment speeds, the percental friction reduction is increased with the increase of SRR. The fact that the friction coefficients in general are higher at the lower speed, Fig. 5, does not indicate a transition to the mixed lubrication regime compared to the higher speeds, but rather an effect of different full film lubrication conditions. A higher entrainment speed will lead to a thicker film and thus lower shear rates. Furthermore, a higher entrainment speed will increase thermal softening of the lubricant, reducing the viscosity and also leading to a

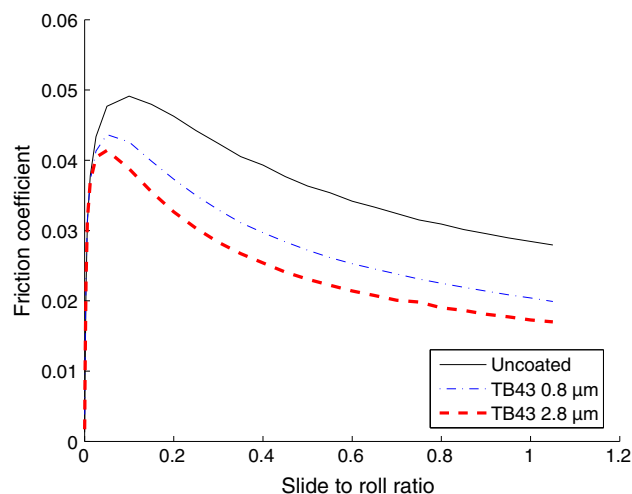


Fig. 6 Friction measurements for squalane at 6.144 m/s entrainment speed and 1.25 GPa of maximum hertzian pressure for uncoated steel and two different thicknesses of the same DLC coating

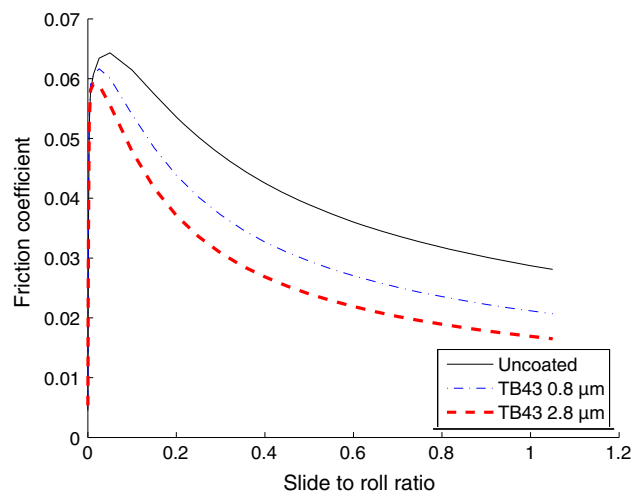


Fig. 7 Friction measurements for squalane at 6.144 m/s entrainment speed and 1.94 GPa of maximum hertzian pressure for uncoated steel and two different thicknesses of the same DLC coating

reduction in friction. When comparing the friction trends at the same speed for both pressures, Figs. 6 and 7, the friction coefficient increases faster with SRR and reaches a higher value for the higher pressure. At higher SRR when thermal softening of the lubricant is dominating the friction behavior, the high pressure case drops more rapidly due to higher heat generation.

4 Discussion

The tribological tests performed in this investigation clearly show the friction-reducing effect of a DLC coating

Table 3 Friction reduction with DLC coatings at SRR = 1.05

Load [N]	Entrainment speed (m/s)	Reduction 0.8 μm (%)	Reduction 2.8 μm (%)
300	6.144	26	41
300	3.145	20	35
80	6.144	29	39
80	3.145	23	37
80	1.611	16	30

in full film EHL, Figs. 5 to 7 and Table 3. The reduction in friction coefficient for the 2.8 μm coating at the highest tested SRRs ranges from 30 % at an entrainment speed of 1.6 m/s and 1.25 GPa of pressure to a reduction of 41 % at an entrainment speed of 6.144 m/s and 1.94 GPa of pressure. For the thinner DLC coating, the same conditions lead to friction reductions of 16 and 26 %. It is apparent that the thicker coating is more effective at reducing friction.

The phenomena of reducing friction with DLC coatings in full film conditions where there are no asperity contacts between the mating surfaces have by several authors been explained as solid–liquid slip [14, 25, 29]. The principle of the theory being that the often assumed no-slip boundary condition between the liquid and the solid is violated. It means that the interaction between the solid and the liquid is not strong enough to resist the shear forces at the interface, and the liquid will thus have a lower velocity than the solid surface. This will in turn reduce shear rates and friction.

If the friction reduction can be explained by the interaction between the surface and the liquid, it must be possible to be determined by utilizing appropriate measurements. Such measurements have included contact angle, surface energy, and spreading parameter. However, results in the literature have been nonconclusive in the sense that some authors have correlated the friction reduction to poor wetting (large contact angle) [13, 23, 25, 29, 41, 42, 49] and sometimes with surface related properties such as hydrophobicity and low surface energy [14, 27]. Recently, Kalin and Polajnar presented a series of studies [26, 27] where they conclude that there is poor correlation between contact angle and friction reduction with surface coatings in full film EHL. On the other hand, they found good correlation between surface energy, and especially the polar part of the surface energy, and friction reduction. They also found good correlation between a spreading parameter, which takes into account both surface and liquid properties, and friction reduction. In this paper, the friction-reducing capabilities of two different thicknesses of the same DLC coatings are investigated with uncoated steel specimens as a reference. As seen in Figs. 5 and 6, the friction reduction is more effective with the thicker coating than the thinner one. However, this difference in friction reduction

between these two coatings cannot be explained by contact angle, surface energy, or spreading parameters. Nor is the surface roughness different between the specimens. In Fig. 4, it can be seen that there is no statistical difference in contact angle between the two coated specimens. The uncoated reference has slightly lower contact angle, but the difference may be within the measurement error. Furthermore, as seen in Fig. 2, there is no statistically significant difference between the two DLC coatings in terms of neither total surface energy, nor the dispersive and polar parts. The surface energies of the coated specimens are, however, lower than the steel reference. Moreover, no significant difference can be seen between the coatings with the calculated spreading parameters in Fig. 3. Even here there is a distinction between the coated specimens and the uncoated steel reference.

This investigation shows that contact angle and surface energy measurements alone are not sufficient to estimate the friction reduction observed with surface coatings in full film EHL. The present authors have earlier [7] hypothesized that the friction reduction obtained in full film EHL may be caused by the low thermal conductivity of certain DLC coatings, and this theory was later validated in another investigation including both experimental measurements and numerical simulations [6]. The mechanism at work in these cases is that applying a thin diamond-like carbon coating to metal surfaces creates an insulating effect that, due to the increased liquid lubricant film temperature at the center of the contact, locally reduces apparent lubricant viscosity and thus friction. The same numerical model was later used to investigate the effect of coating thickness and thermal properties of the coatings on friction reduction [19] with results in line with those obtained experimentally in this paper.

The idea that thermal properties of the specimens have an influence on film shape and friction is not new. The concept of a temperature-viscosity wedge caused by specimens with widely different thermal conductivities was introduced by Cameron in the 1960s [10, 11] and has been discussed by several authors [30].

It is therefore likely that some of the inconsistencies between contact angles and/or surface energies and friction reduction achieved in full film EHL may be explained by the fact that solid–liquid slip alone cannot explain or describe the phenomena. In fact, under certain conditions, the thermally insulating effects of the coatings are dominating, or possibly even the only cause to the friction reduction. In this investigation, since there is no significant difference between contact angle and surface energy of the two coating thicknesses, the difference in friction reduction may solely depend on different thermal properties due to the different thicknesses of the coatings. However, it is more uncertain if the friction reduction achieved with the

coatings compared to the uncoated reference is only due to thermal insulation, or if a smaller part of the friction reduction is also due to solid–liquid slip.

The influence of surface roughness on solid–liquid slip has been discussed by several authors, where many of them have concluded that for slip to occur, the surfaces have to be very smooth [12, 39, 41, 42, 49], typically 6–12 nm RMS. The critical roughness is most likely depending on the size of the molecules of the liquid used [24, 36, 38]. Pearson and Petrie [36] mean that no slip can occur when the molecular size is smaller than the wall roughness scale. However, it is not necessarily so that as smooth a surface as possible will lead to the greatest amount of slip. At relatively low roughness (below 15 nm), it has been shown that RMS roughnesses of 0.7 and 4.0 nm produced less slip than a 12.2 nm surface [9]. It should, however, be mentioned that the roughness in this case was not only different in amplitude, but also produced with different geometries. That an optimized roughness is superior to very smooth surfaces in some cases may be apparent by considering solutions from nature such as lotus leaves [3, 4]. In nature, for instance low wettability is created by clever use of surface texturing.

Moreover, most of the investigations on solid–liquid slip are performed at atmospheric pressure or hydrodynamic pressure and may therefore not be directly applicable on EHL. Solid–liquid slip has been reported to be reduced with pressure in the hydrodynamic pressure range [44, 45], but also observed to increase with pressure in EHL [32]. In favor for solid–liquid slip in EHL is amplitude reduction [17, 33] that describes elastic deformation of the roughness inside the high pressure contact. Studies show that the roughness reduction is dependent on several factors, such as entrainment speed, slide to roll ratio, and pressure, and that long wavelengths are compressed more than short wavelengths. This means that the actual roughness inside the high pressure region may, depending on the roughness parameters and running conditions, be smoother than outside of the contact. This would at least according to Pearson and Petrie be beneficial for solid–liquid slip.

To the author's knowledge, only a few studies have observed solid–liquid slip in EHL [18, 32, 47], and they have all used relatively smooth surfaces (below 12 nm). The liquids they used are either polyphenyl ether (5P4E) which has very high surface tension and is known to show poor wetting at metal surfaces, or high molecular weight polybutene. It is still to be elucidated whether solid–liquid slip can still be observed with the use of surfaces and lubricants more often encountered in machine elements such as ball bearings and gears. Studies that indirectly indicate solid–liquid slip as a consequence of reduced friction in full film EHL may, in fact, as indicated by this study, be an effect of thermal insulation, or a combination between thermal insulation and solid–liquid slip.

5 In Conclusion

This paper shows that measurements of contact angle, surface energy, or spreading parameter alone are not sufficient to estimate the full film EHD friction reduction capability of a surface coating. Friction tests were carried out in a ball-on-disk machine with specimens coated with the same DLC coating, but with different thicknesses, and compared to uncoated specimens, all with the same surface roughness. The DLC-coated surfaces showed a reduction in friction in all tested cases compared to the uncoated specimens. However, the thicker DLC coating provided substantially lower friction than the thinner coating. Contact angle measurements were carried out with reference fluids and the test fluid to calculate surface energy and spreading parameter for the test combinations. No significant differences were found between the two coating thicknesses although their friction reduction effects were substantially different. The difference in friction reduction between the coatings is attributed to the fact that the thicker coating has a greater thermal insulating effect than the thinner coating.

Acknowledgments The authors wish to thank IonBond AB for providing the DLC coatings used in the tests and the Swedish Foundation for Strategic Research (ProViking) and VR (Swedish Research Council) for financial support.

Open Access This article is distributed under the terms of the Creative Commons Attribution License which permits any use, distribution, and reproduction in any medium, provided the original author(s) and the source are credited.

References

- Bair, S.: Reference liquids for quantitative elastohydrodynamics. *Tribol. Lett.* **22**(2), 197–206 (2006). doi:[10.1007/s11249-006-9083-y](https://doi.org/10.1007/s11249-006-9083-y)
- Balandin, A., Shamsa, M., Liu, W., Casiraghi, C., Ferrari, A.: Thermal conductivity of ultrathin tetrahedral amorphous carbon films. *Appl. Phys. Lett.* **93**(4), 043115 (2008). doi:[10.1063/1.2957041](https://doi.org/10.1063/1.2957041)
- Bhushan, B.: Biomimetics: lessons from nature—an overview. *Philos. Trans. R. Soc. A Math. Phys. Eng. Sci.* **367**(1893), 1445–1486 (2009). doi:[10.1098/rsta.2009.0011](https://doi.org/10.1098/rsta.2009.0011)
- Bhushan, B., Jung, Y.C.: Natural and biomimetic artificial surfaces for superhydrophobicity, self-cleaning, low adhesion and drag reduction. *Prog. Mater. Sci.* **56**(1), 1–108 (2011). doi:[10.1016/j.pmatsci.2010.04.003](https://doi.org/10.1016/j.pmatsci.2010.04.003)
- Björling, M., Habchi, W., Bair, S., Larsson, R., Marklund, P.: Towards the true prediction of ehl friction. *Tribol. Int.* **66**, 19–26 (2013). doi:[10.1016/j.triboint.2013.04.008](https://doi.org/10.1016/j.triboint.2013.04.008)
- Björling, M., Habchi, W., Bair, S., Larsson, R., Marklund, P.: Friction reduction in elastohydrodynamic contacts by thin-layer thermal insulation. *Tribol. Lett.* **54**(2), 477–486 (2014). doi:[10.1007/s11249-013-0286-8](https://doi.org/10.1007/s11249-013-0286-8)
- Björling, M., Isaksson, P., Marklund, P., Larsson, R.: The influence of dlc coating on ehl friction coefficient. *Tribol. Lett.* **47**(2), 285–294 (2012). doi:[10.1007/s11249-012-9987-7](https://doi.org/10.1007/s11249-012-9987-7)
- Björling, M., Larsson, R., Marklund, P., Kassfeldt, E.: Elastohydrodynamic lubrication friction mapping—the influence of

- lubricant, roughness, speed, and slide-to-roll ratio. *Proc. Inst. Mech. Eng. Part J J. Eng. Tribol.* **225**(7), 671–681 (2011). doi:[10.1177/1350650111403363](https://doi.org/10.1177/1350650111403363)
9. Bonaccorso, E., Butt, H.J., Craig, V.S.J.: Surface roughness and hydrodynamic newtonian fluid in a completely wetting system. *Phys. Rev. Lett.* **90**(14), 144501/1–144501/4 (2003). doi:[10.1103/PhysRevLett.90.144501](https://doi.org/10.1103/PhysRevLett.90.144501)
 10. Cameron, A.: Hydrodynamic lubrication of rotating disks in pure sliding, a new type of oil film formation. *Inst. Pet.* **37**, 471–786 (1951)
 11. Cameron, A.: The viscosity wedge. *ASLE Trans.* **1**(2), 243–248 (1958). doi:[10.1080/05698195808972337](https://doi.org/10.1080/05698195808972337)
 12. Choo, J.H., Glovnea, R.P., Forrest, A.K., Spikes, H.A.: A low friction bearing based on liquid slip at the wall. *J. Tribol.* **129**(3), 611–620 (2007). doi:[10.1115/1.2736704](https://doi.org/10.1115/1.2736704)
 13. Choo, J.H., Spikes, H.A., Ratoi, M., Glovnea, R., Forrest, A.: Friction reduction in low load hydrodynamic lubrication with a hydrophobic surface. *Tribol. Int.* **40**(2), 154–159 (2007). doi:[10.1016/j.triboint.2005.09.006](https://doi.org/10.1016/j.triboint.2005.09.006)
 14. Evans, R.D., Cogdell, J.D., Richter, G.A.: Traction of lubricated rolling contacts between thin-film coatings and steel. *Tribol. Trans.* **52**(1), 106–113 (2009). doi:[10.1080/10402000802180144](https://doi.org/10.1080/10402000802180144)
 15. Fan, C.W., Lee, S.C.: Surface free energy effects in sputter-deposited wnx films. *Mater. Trans.* **48**(9), 2449–2453 (2007). doi:[10.2320/matertrans.MRA2007095](https://doi.org/10.2320/matertrans.MRA2007095)
 16. Fowkes, F.M.: Attractive forces at interfaces. *J. Ind. Eng. Chem.* **56**(12), 40–52 (1964). doi:[10.1021/ie50660a008](https://doi.org/10.1021/ie50660a008)
 17. Greenwood, J.A., Morales-Espejel, G.E.: The behaviour of transverse roughness in EHL contacts. *Proc. Inst. Mech. Eng. Part J J. Eng. Tribol.* **208**(2), 121–132 (1994)
 18. Guo, F., Wong, P.L., Geng, M., Kaneta, M.: Occurrence of wall slip in elastohydrodynamic lubrication contacts. *Tribol. Lett.* **34**(2), 103–111 (2009). doi:[10.1007/s11249-009-9414-x](https://doi.org/10.1007/s11249-009-9414-x)
 19. Habchi, W.: A numerical model for the solution of thermal elastohydrodynamic lubrication in coated circular contacts. *Tribol. Int.* **73**, 57–68 (2014). doi:[10.1016/j.triboint.2014.01.002](https://doi.org/10.1016/j.triboint.2014.01.002)
 20. Habchi, W., Eyheramendy, D., Bair, S., Vergne, P., Morales-Espejel, G.: Thermal elastohydrodynamic lubrication of point contacts using a newtonian/generalized newtonian lubricant. *Tribol. Lett.* **30**(1), 41–52 (2008). doi:[10.1007/s11249-008-9310-9](https://doi.org/10.1007/s11249-008-9310-9)
 21. Habchi, W., Eyheramendy, D., Vergne, P., Morales-Espejel, G.: A full-system approach of the elastohydrodynamic line/point contact problem. *ASME J. Tribol.* **130**(021501), 1–10 (2008). doi:[10.1115/1.2842246](https://doi.org/10.1115/1.2842246)
 22. Habchi, W., Vergne, P., Bair, S., Andersson, O., Eyheramendy, D., Morales-Espejel, G.E.: Influence of pressure and temperature dependence of thermal properties of a lubricant on the behaviour of circular tehd contacts. *Tribol. Int.* **43**(10), 1842–1850 (2010). doi:[10.1016/j.triboint.2009.10.002](https://doi.org/10.1016/j.triboint.2009.10.002)
 23. Hild, W., Opitz, A., Schaefer, J.A., Scherge, M.: The effect of wetting on the microhydrodynamics of surfaces lubricated with water and oil. *Wear* **254**(9), 871–875 (2003). doi:[10.1016/S0043-1648\(03\)00238-2](https://doi.org/10.1016/S0043-1648(03)00238-2)
 24. Jabbarzadeh, A., Atkinson, J.D., Tanner, R.I.: Effect of the wall roughness on slip and rheological properties of hexadecane in molecular dynamics simulation of couette shear flow between two sinusoidal walls. *Phys. Rev. E* **61**(1), 690–699 (2000). doi:[10.1103/PhysRevE.61.690](https://doi.org/10.1103/PhysRevE.61.690)
 25. Jahanmir, S., Hunsberger, A., Heshmat, H.: Load capacity and durability of h-dlc coated hydrodynamic thrust bearings. *J. Tribol.* **133**(3), 031301 (2011). doi:[10.1115/1.4003997](https://doi.org/10.1115/1.4003997)
 26. Kalin, M., Polajnar, M.: The correlation between the surface energy, the contact angle and the spreading parameter, and their relevance for the wetting behaviour of dlc with lubricating oils. *Tribol. Int.* **66**, 225–233 (2013). doi:[10.1016/j.triboint.2013.05.007](https://doi.org/10.1016/j.triboint.2013.05.007)
 27. Kalin, M., Polajnar, M.: The effect of wetting and surface energy on the friction and slip in oil-lubricated contacts. *Tribol. Lett.* **52**(2), 185–194 (2013). doi:[10.1007/s11249-013-0194-y](https://doi.org/10.1007/s11249-013-0194-y)
 28. Kalin, M., Polajnar, M.: The wetting of steel, dlc coatings, ceramics and polymers with oils and water: The importance and correlations of surface energy, surface tension, contact angle and spreading. *Appl. Surf. Sci.* **293**, 97–108 (2014). doi:[10.1016/j.apsusc.2013.12.109](https://doi.org/10.1016/j.apsusc.2013.12.109)
 29. Kalin, M., Velkavrh, I., Vižintin, J.: The stribeck curve and lubrication design for non-fully wetted surfaces. *Wear* **267**(5–8), 1232–1240 (2009). doi:[10.1016/j.wear.2008.12.072](https://doi.org/10.1016/j.wear.2008.12.072)
 30. Kaneta, M., Yang, P.: Effects of the thermal conductivity of contact materials on elastohydrodynamic lubrication characteristics. *Proc. Inst. Mech. Eng. Part C J. Mech. Eng. Sci.* **224**(12), 2577–2587 (2010). doi:[10.1243/09544062JMES2146](https://doi.org/10.1243/09544062JMES2146)
 31. Kim, J.W., Yang, H.S., Jun, Y.H., Kim, K.C.: Interfacial effect on thermal conductivity of diamond-like carbon films. *J. Mech. Sci. Tech.* **24**(7), 1511–1514 (2010). doi:[10.1007/s12206-010-0416-2](https://doi.org/10.1007/s12206-010-0416-2)
 32. Li, X.M., Guo, F., Wong, P.L.: Shear rate and pressure effects on boundary slippage in highly stressed contacts. *Tribol. Int.* **59**, 147–153 (2013). doi:[10.1016/j.triboint.2012.06.030](https://doi.org/10.1016/j.triboint.2012.06.030)
 33. Lubrecht, A.A., Venner, C.H.: Elastohydrodynamic lubrication of rough surfaces. *Proc. Inst. Mech. Eng. Part J J. Eng. Tribol.* **213**, 397–403 (1999)
 34. Lugscheider, E., Bobzin, K.: Wettability of pvd compound materials by lubricants. *Surf. Coat. Tech.* **165**(1), 51–57 (2003). doi:[10.1016/S0257-8972\(02\)00724-7](https://doi.org/10.1016/S0257-8972(02)00724-7)
 35. Owens, D.K., Wendt, R.: Estimation of the surface free energy of polymers. *J. App. Poly. Sci.* **13**(8), 1741–1747 (1969). doi:[10.1002/app.1969.070130815](https://doi.org/10.1002/app.1969.070130815)
 36. Pearson, J.R.A., Petrie, C.J.S.: *Polymer systems: deformation and flow*. Macmillan, London (1968)
 37. Pit, R., Hervet, H., Léger, L.: Friction and slip of a simple liquid at a solid surface. *Tribol. Lett.* **7**(2–3), 147–152 (1999). doi:[10.1023/A:1019161101812](https://doi.org/10.1023/A:1019161101812)
 38. Pit, R., Hervet, H., Léger, L.: Direct experimental evidence of slip in hexadecane: solid interfaces. *Phys. Rev. Lett.* **85**(5), 980–983 (2000). doi:[10.1103/PhysRevLett.85.980](https://doi.org/10.1103/PhysRevLett.85.980)
 39. Sarkar, K., Prosperetti, A.: Effective boundary conditions for stokes flow over a rough surface. *J. Fluid Mech.* **316**, 223–240 (1996). doi:[10.1017/S0022112096000511](https://doi.org/10.1017/S0022112096000511)
 40. Shamsa, M., Liu, W., Balandin, A., Casiraghi, C., Milne, W., Ferrari, A.: Thermal conductivity of diamond-like carbon films. *Appl. Phys. Lett.* **89**(16), 161921 (2006). doi:[10.1063/1.2362601](https://doi.org/10.1063/1.2362601)
 41. Spikes, H.A.: The half-wetted bearing. part 1: extended reynolds equation. *Proc. Inst. Mech. Eng. Part J J. Eng. Tribol.* **217**(1), 1–14 (2003). doi:[10.1243/135065003321164758](https://doi.org/10.1243/135065003321164758)
 42. Spikes, H.A.: The half-wetted bearing. part 2: potential application in low load contacts. *Proc. Inst. Mech. Eng. Part J J. Eng. Tribol.* **217**(1), 15–26 (2003). doi:[10.1243/135065003321164776](https://doi.org/10.1243/135065003321164776)
 43. Swartz, E.T., Pohl, R.O.: Thermal boundary resistance. *Rev. Mod. Phys.* **61**(3), 605–668 (1989). doi:[10.1103/RevModPhys.61.605](https://doi.org/10.1103/RevModPhys.61.605)
 44. Tang, H.S., Kalyon, D.M.: Unsteady circular tube flow of compressible polymeric liquids subject to pressure-dependent wall slip. *J. Rheol.* **52**(2), 507–525 (2008). doi:[10.1122/1.2837104](https://doi.org/10.1122/1.2837104)
 45. Tanner, R.I.: *Engineering Rheology*. Clarendon Press, Oxford (1985)
 46. Thompson, P., Troian, S.: A general boundary condition for liquid flow at solid surfaces. *Nat.* **389**(6649), 360–362 (1997). doi:[10.1038/38686](https://doi.org/10.1038/38686)
 47. Wong, P., Li, X., Guo, F.: Evidence of lubricant slip on steel surface in ehl contact. *Tribol. Int.* **61**, 116–119 (2013). doi:[10.1016/j.triboint.2012.12.009](https://doi.org/10.1016/j.triboint.2012.12.009)

48. Xu, H.: Development of a generalized mechanical efficiency prediction methodology for gear pairs. Ph.D. thesis, Graduate School of The Ohio State University (2005)
49. Zhu, Y., Granick, S.: Rate-dependent slip of newtonian liquid at smooth surfaces. *Phys. Rev. Lett* **87**(9), 961051–961054 (2001). doi:[10.1103/PhysRevLett.87.096105](https://doi.org/10.1103/PhysRevLett.87.096105)
50. Zhu, Y., Granick, S.: Limits of hydrodynamic no-slip boundary condition. *Phys. Rev. Lett.* **88**(10), 1061021–1061024 (2002). doi:[10.1103/PhysRevLett.88.106102](https://doi.org/10.1103/PhysRevLett.88.106102)